Chapter 4

Jatropha curcas oil based alkyd/epoxy resin/expanded graphite (EG) reinforced bio-composite: Evaluation of the thermal, mechanical, and flame retardant properties

GRAPHICAL ABSTRACT

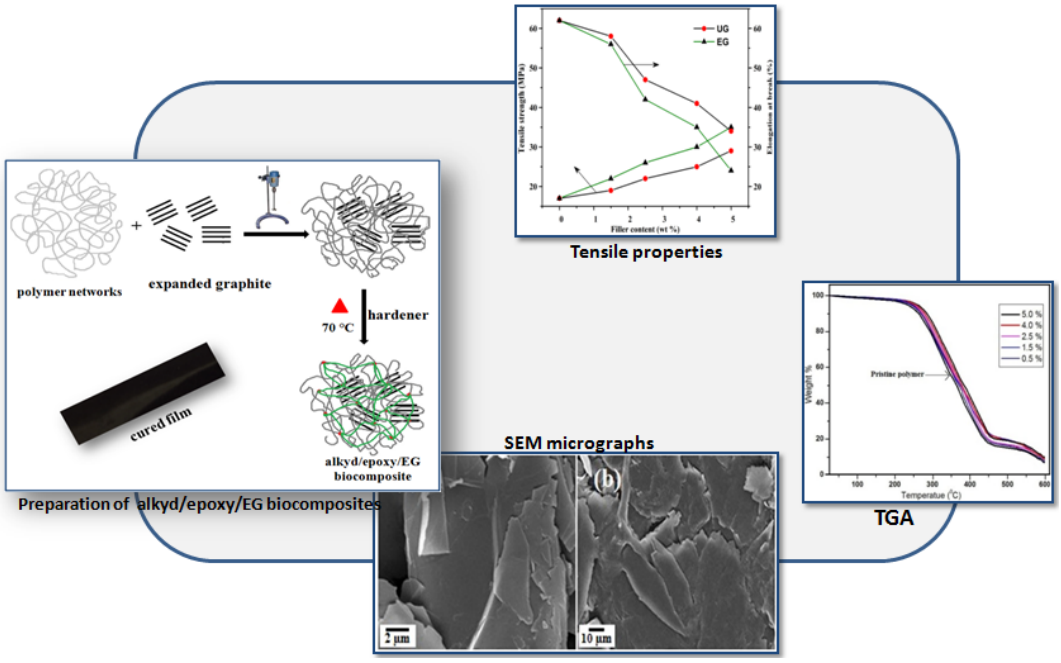

4.1 Introduction

In recent years, biopolymers have received a great scientific attention because of more environmentally aware consumer society, high rate of depletion of petroleum resources and increased cost of crude oil. In general, plant oils have attracted much attention as raw materials for the preparation of resins and composite materials to replace the conventional petro-chemical based polymers. Plant oils such as castor, linseed, tung oil, soybean oil, safflower oil, sunflower oil, canola oil have been used in many products like paints, coatings, soaps, lubricants, bioplastics, etc.[1–4] Recently Wang et al. reported the synthesis and characterization of novel soybean-oil-based elastomers with favourable processability and tunable properties.[5]

Vegetable oil based alkyd resins have a number of advantages, including versatility in structure and properties, overall low cost and ease of application. In contrast to the difficulty in preparing low molecular weight acrylic resins with at least two hydroxyl groups, the synthesis of alkyd resins with two or more hydroxyl groups is relatively easy.[6] However, they suffer some major drawbacks such as low alkali resistance, low mechanical strength, low hardness, and low thermal stability and long curing time. To improve these drawbacks of vegetable oil based alkyd resins, blending with other suitable resins, such as epoxy resin, amino resin, silicone resin and ketonic resin can be performed.[7] The better compatibility comes from the relatively low viscosity of the resin and from its structure, which contains a relatively polar and aromatic backbone and aliphatic side chains with low polarity.[8,9]

A part of this chapter is published

P. Gogoi, M. Boruah, C. Bora, S.K. Dolui, *Progress in Organic Coatings* 2014, 77(1), 87-93.

Polymer based nanocomposites containing multifunctional nanoparticles such as silicates, fullerenes, carbon nanotubes, and graphene sheets are being developed with enhanced thermal, mechanical, electrical, flame retardant properties.[10–12] The most extensively studied polymer nanocomposites so far are those based on layered-silicate clays because of their availability, low cost and they can impart mechanical strength, thermal, gas barrier, and flame retardant properties.[13–15]

The CNTs filled bionanocomposites were proved to exhibit remarkable performances in terms of mechanical, electrical, flame retardant, and gas barrier properties. But the high cost of CNTs limits their uses in industrial sectors. In this regard low cost graphite can be an alternative to make polymer composites. Graphite consists of graphene nanosheets and has thermal and electrical properties usually affiliated with metals. Recently, a number of studies have been carried out on dispersion of expanded graphite (EG) and exfoliated graphite nanoplatelets (GNP) in commercial polymers such as poly(phenylene sulfide), polyamide 6, epoxy resins, poly(methyl methacrylate) or polypropylene.[16,17] The PA-6/graphite nanocomposites showed similar composite structures i.e. comparable filler dispersions when compared to PA-6/montmorillonite clay nanocomposites with superior flame retardant properties.[18] Nanocomposites reinforced with 1 wt % of EG showed a 15% improvement of elastic modulus over pure epoxy. This could be attributed to the in situ formation of graphite nanosheets as well as uniform dispersion and exfoliation of graphite nanosheets.[19]

However, preparation of biocomposites based on oil modified alkyd resins and EG has not been done so far. In this regard our main aim is to present preparation of EG based biocomposites using polymer matrix that is renewable and environmentally benign. To obtain “green” biocomposites with specific properties, EG was mixed homogeneously by mechanical mixing to the blend of *Jatropha curcas* oil based alkyd and epoxy resin. The effect of EG on thermal, mechanical, and flame retardant properties of the resulting biocomposites was evaluated.

4.2 Experimental

4.2.1 Materials

Jatropha oil based alkyd resin with 100% phthalic anhydride was prepared by the method described in Chapter 2. Epoxy resin (epoxy equivalent weight: 170–180 g/eq) and hardener poly(amido amine), methyl ethyl ketone peroxide (MEKP), and cobalt octoate of commercial grade (Kumud Enterprises, Kharagpur, West Bengal, India) were used as received. The natural graphite flake of size <20 micron (Shanker Graphites and Chemical, New Delhi, India), hydrochloric acid, sulphuric acid, nitric acid, phthalic anhydride, and potassium persulphate ($K_2S_2O_8$) were of analytical reagent grade chemicals (Merck) were used as received.

4.2.2 Preparation of jatropha oil based alkyd resin

In a typical method a three necked round bottom flask equipped with a mechanical stirrer, a thermometer and a nitrogen gas inlet was charged with 32.68 g (0.04 mol) of jatropha oil, 7.36 g (0.08 mol) of glycerol and 0.05 wt % of PbO with continuous stirring. The mixture was heated upto 230 °C for 45–60 min until monoglyceride was formed. Formation of monoglyceride was confirmed by its solubility in methanol (monoglyceride:methanol = 1:3, v/v) at room temperature. Then the reaction mixture was cooled to 125 °C and 17.77 g (0.12 mol) of phthalic anhydride in the form of fine powder with 1.98 g of excess glycerol (27%) was added. Again, the reaction temperature was raised to 230 °C until it reached acid value in the range of 20–40 mg KOH/g.[20]

4.2.3 Preparation of expanded graphite (EG)

Expanded graphite (EG) was prepared as reported elsewhere.[17,21] A mixture of concentrated H_2SO_4 and HNO_3 (4:1, v/v) was mixed with natural graphite flake at ambient temperature. The reaction mixture was stirred continuously for 16 h. The acid treated natural graphite was washed thoroughly with distilled water until neutral pH was attained. It was then dried in an oven at 100 °C to remove any remaining water. The dried particles were heated at 1050 °C for 15 s to obtain the expanded graphite particles.

4.2.4 Preparation of alkyd/epoxy/EG biocomposites

For the preparation of alkyd/epoxy/EG biocomposites, jatropha oil modified alkyd and epoxy resins were mixed at predetermined ratios of 50:50 (w/w) along with different concentrations of EG (0.5, 1.5, 2.5, 4, and 5 wt %). In each case poly(amido amine) was added 50% by weight with respect to the epoxy resin. MEKP and cobalt octoate was added 4 and 2 wt %, respectively with respect to the alkyd resin for the curing of the unsaturated alkyd resins. Here, MEKP acts as an initiator and cobalt octoate accelerates the reaction rate.[8] The mixture was mixed under continuous agitation by mechanical stirring to get homogeneous dispersion of the EG within the polymer matrix (Scheme 4.1). Afterwards, the mixture was casted on a Teflon coated plate by an applicator maintaining the thickness uniformly (0.4 mm) and allowed to cure in an oven at 70 °C. The curing time of the different biocomposites was recorded.

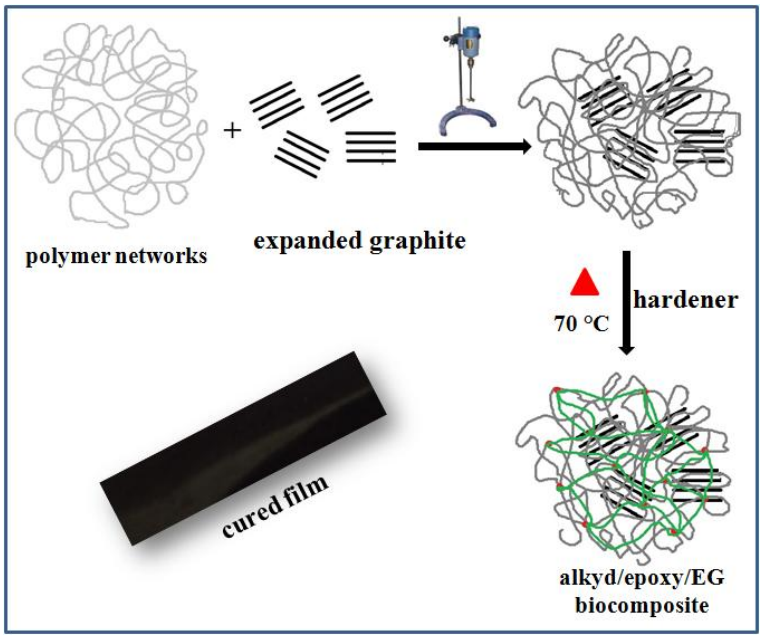

Scheme 4.1: Schematic representation of the preparation of alkyd/epoxy/EG biocomposites.

4.3 Instruments and methods

4.3.1 Fourier transform infrared spectrometer (FT-IR)

Fourier transform infrared spectra were obtained by using Nicolet Impact-410 IR spectrometer (USA), equipped with KBr plate, and the spectra were recorded in transmission mode in the range of 4000–500 cm^{-1} with a nominal resolution of 4 cm^{-1}.

4.3.2 X-ray diffractometer (XRD)

Powder X-Ray diffraction (XRD) data were collected on a Rigaku Miniflex X-ray diffractometer (Tokyo, Japan) with Cu Kα radiation (λ=0.15418 Å) at 30 kV and 15 mA with a scanning rate of 0.05° s^{-1} in a 2θ ranges from 20 to 80°.

From the 2θ value for the reflections, d values were calculated using Bragg's equation.

$$n\lambda = 2d\sin\theta \qquad \text{(Eqn. 4.1)}$$

where, 'n' is an integer, 'λ' is the X-ray wavelength, 'd' is the distance between crystal lattice planes and 'θ' is the diffraction angle.

4.3.3 Scanning electron microscopy (SEM)

The surface morphology of some of the prepared sample was studied by scanning electron microscope (Model JSM-6390LV, JEOL, Japan) at an accelerating voltage of 5–15 kV. The surface of the sample was platinum coated before observation.

4.3.4 Transmission electron microscopy (TEM)

Transmission electron microscopy (TEM) is a microscopy technique whereby a beam of electrons is transmitted through an ultra thin specimen, interacting with the specimen as it passes through. An image is formed from the interaction of the electrons transmitted through the specimen; the image is magnified and focused onto an imaging device. TEM is capable of imaging at a significantly higher resolution than light microscopes, owing to the small de Broglie wavelength of electrons. This enables to examine fine detail of even as small as a single column of atoms, which is tens of thousands times smaller than the smallest resolvable object in a light microscope.

The study of the dispersion and intercalation of EG in the biocomposite was carried out by using transmission electron microscope (JEOL, JEM 2100) at an accelerating voltage of 200 kV.

4.3.5 Thermogravimetric analysis (TGA)

Thermogravimetric analysis of the biocomposite samples were carried out by using Shimazdu TGA 50, thermal analyzer under the nitrogen flow rate of 30 mL min^{-1} at the heating rate of 10 °C min^{-1} from 25-600 °C.

4.3.6 Mechanical property

Mechanical properties of biocomposite films such as Young's modulus, tensile strength, and strain at break were examined using a universal testing machine (UTM, Zwick, Z010) at ambient temperature. Experiments were performed with a cross-head speed of 50 mm min^{-1} at 25 °C. The sample dimensions were 10 mm x 5 mm x 0.4 mm, and the results were the averages of three measurements.

4.3.7 Limiting oxygen index (LOI)

Limiting oxygen index (LOI) is defined as the minimum concentrations of oxygen, expressed as a percentage, in a flowing mixture of oxygen and nitrogen that will support catch fire of a material initially at room temperature. The specimens were cut into 100 mm × 6 mm × 3 mm (longitudinal x tangential x radial) according to ASTM-D 2863 and placed vertically in the flammability tester (S.C. Dey Co., Kolkata). The volume of nitrogen gas and that of oxygen gas were kept initially at a maximum and minimum level. Now, the volume of nitrogen gas was decreased and that of oxygen gas was increased gradually. However, the total volume of the gas mixture (N_2 + O_2) was kept fixed at 18 cc during the experiment. The ratio of N_2 and O_2 at which the sample continued to burn was recorded for at least 30 s and the LOI value is calculated by following equation:

$$\text{LOI} = \left[\frac{\text{Volume of } O_2}{\text{Volume of } O_2 + \text{Volume of } N_2}\right] \text{x } 100 \qquad \text{(Eqn. 4.2)}$$

4.4 Results and discussion

4.4.1 FT-IR analysis

The FT-IR spectra of EG, alkyd/epoxy blend, and alkyd/epoxy/EG biocomposite are shown in Fig. 4.1. In FT-IR spectra of EG (Fig. 4.1a), some new peaks are observed at lower wave number in between 400 and 800 cm^{-1} due to the C–H outer bending vibration, C–H in plane bending and out-of-plane C–H wagging.[22,23] The peak at about 3476 cm^{-1} is attributed to the O–H stretching vibration of the hydroxyl groups present on the EG surface. The peak at around 1650 cm^{-1} is of the C–O stretching of carboxyl functional groups. During intercalation of natural graphite by strong acids some of the carbon double

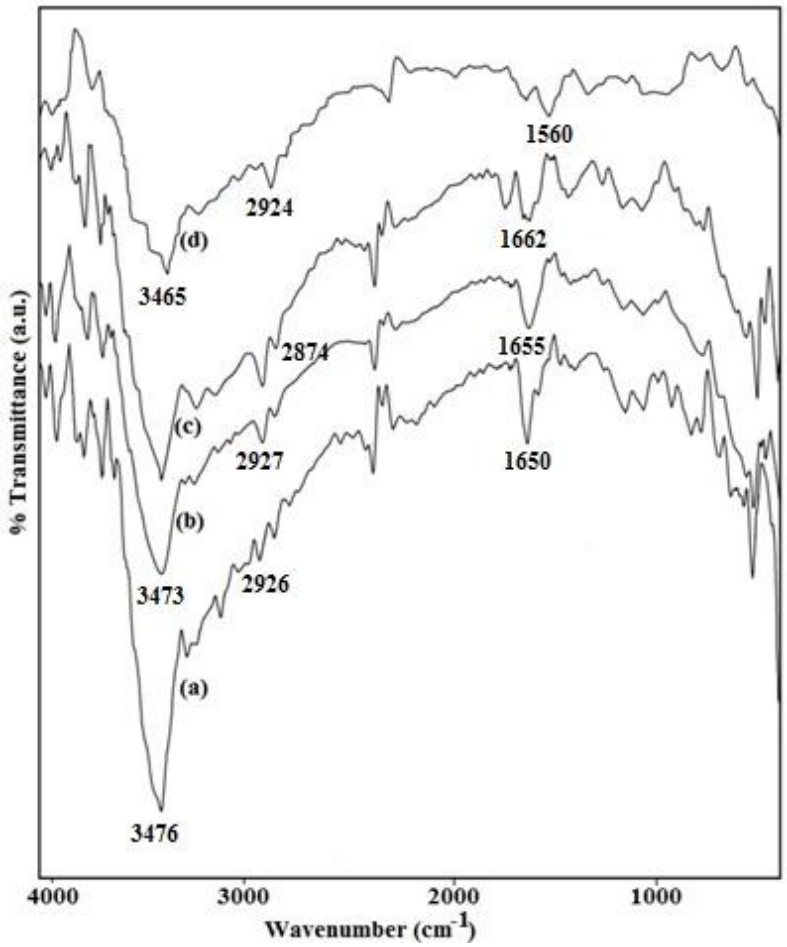

Fig. 4.1: FT-IR spectra of EG (a), alkyd/epoxy blend (b), biocomposites with 2.5 (c) and 5 (d) wt % EG.

bonds are oxidized, which leads to the formation of oxygen containing functional groups like, carboxylic and hydroxyl on exfoliated graphite surface. These functional groups can facilitate the physical and chemical interactions with the polar sites of the polymer matrix.[24] In the biocomposite peak at 1560 cm^{-1} is of the C–C–C symmetric stretching vibration and at 1655 cm^{-1} is attributed to stretching frequency of C=O in keto form. The broad absorption band at 3400 cm^{-1} indicates O–H stretching vibration, whereas the band at 2924 cm^{-1} is due to the stretching of the C–H bonds. Compared to the neat polymer matrix and EG, the shifting of O–H stretching to lower frequency in the biocomposite indicates the strong interaction of hydroxyl groups with other polar functionalities. This interaction imparts mechanical strength of the biocomposite to a remarkable extent.

4.4.2 X-ray diffraction analysis

The X-ray diffraction patterns for neat polymer and biocomposites with 0.5–5 wt % EG are shown in the Fig. 4.2. The EG exhibited a sharp peak at 2θ = 26.40° with a d-spacing of 0.346 nm (Fig. 4.2a) and the neat polymer shows a broad peak (Fig. 4.2f). The

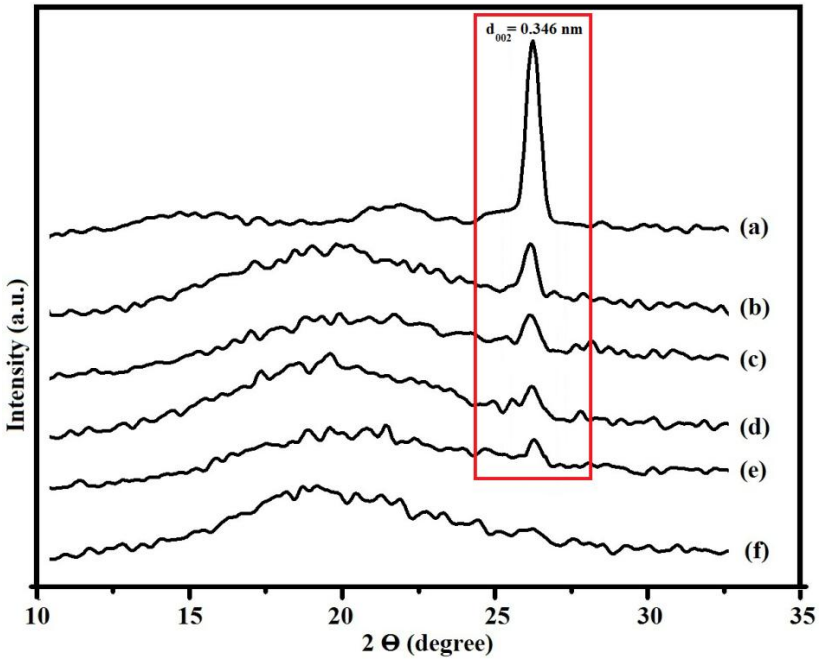

Fig. 4.2: XRD patterns of EG (a), biocomposites with 5 (b), 4 (c), 2.5 (d) and 1.5 (e) wt % EG, and neat polymer (f).

occurrence of the peak near at 2θ = 26.40° for the biocomposites confirms successful incorporation of EG within the polymer matrix.[19] It should be noted that the intensity of the peak is observed to be decreased gradually with decrease in EG content in the biocomposites. The higher intensity for higher EG content can be attributed to the higher number of graphite layers. Since there is no significant change of 2θ peaks, indicating that there is no change in the gallery spaces of EG layers during the mixing process.[21]

4.4.3 Morphology study

4.4.3.1 SEM analysis

The differences in microstructures between natural graphite and EG can be seen from the SEM micrographs (Fig. 4.3). The layered structures of EG is distinctly observed in higher magnifications (Fig. 4.3b and c). This is due to opening of planar carbon networks wedged at the edge surface of crystallite by surface groups as a consequence of oxidation. In EG, the interlayer spacing is separated by increased distance leading into a porous structure consisting of numerous graphite sheets.[25]

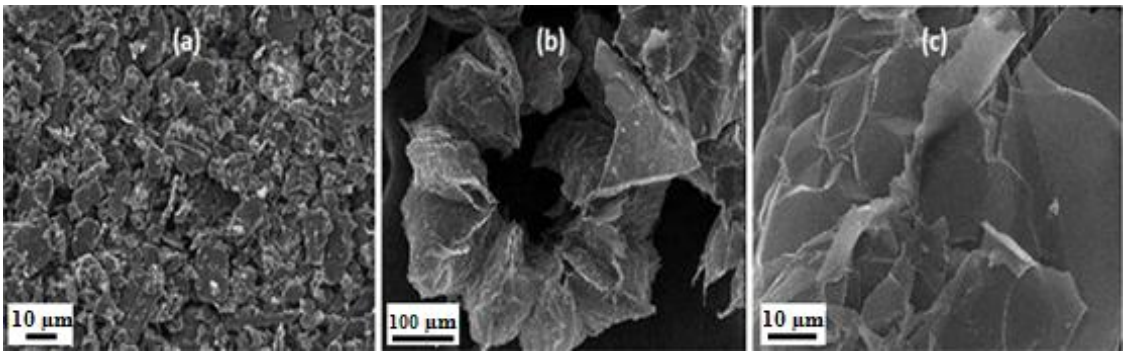

Fig. 4.3: SEM micrographs of natural graphite (a), and EG (b) and (c) at different magnifications.

SEM micrographs of the biocomposite (Fig. 4.4) suggest the uniform dispersion of EG sheets in the polymer blend matrix. These also support the miscibility of EG sheets in the polymer matrix. It implies that EG is compatible with alkyd/epoxy resin blend. The layered structure of EG in the biocomposites is clearly observed in the SEM micrograph with different weight percentage of EG loading. So, from the morphological study successfully incorporation of EG in the polymer blend matrix can be confirmed.

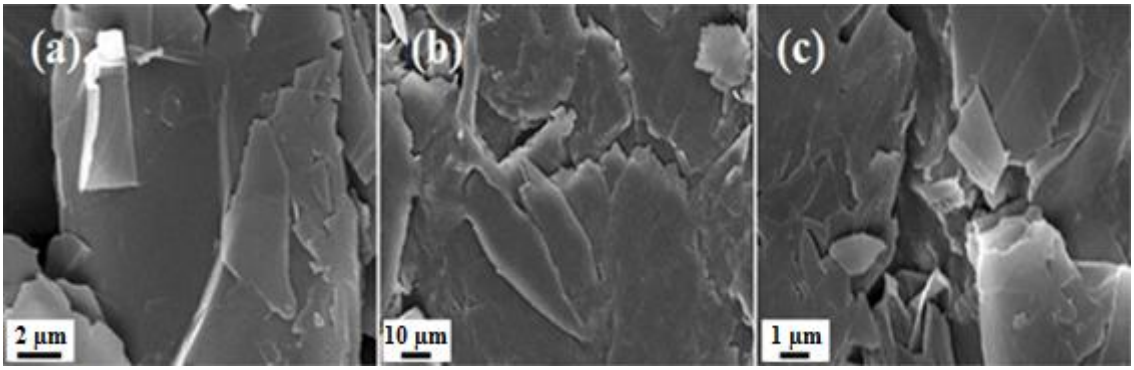

Fig.4.4: SEM micrographs of the biocomposites with (a) 2.5, and (b) and (c) 5 wt % EG.

4.4.3.2 TEM analysis

Fig. 4.5 presents the TEM micrographs of the alkyd/epoxy/EG biocomposites. It is observed that the EG sheets are composed of thinner sheets with thickness of 9–13 nm, with spaces between them. These spaces are one of the reasons for the low apparent density of the EG.[21] It is observed from the TEM micrographs that the graphite layers are dispersed homogeneously within the polymer matrix and not aligned any more. In addition, the graphite layers in ordered stacks are observed in the biocomposites. The polymer chains get intercalated into the layers of EG and the lattices still retain their layered structure in the composites. Thus, the TEM and XRD study confirms the formation of the alkyd/epoxy/EG biocomposites.

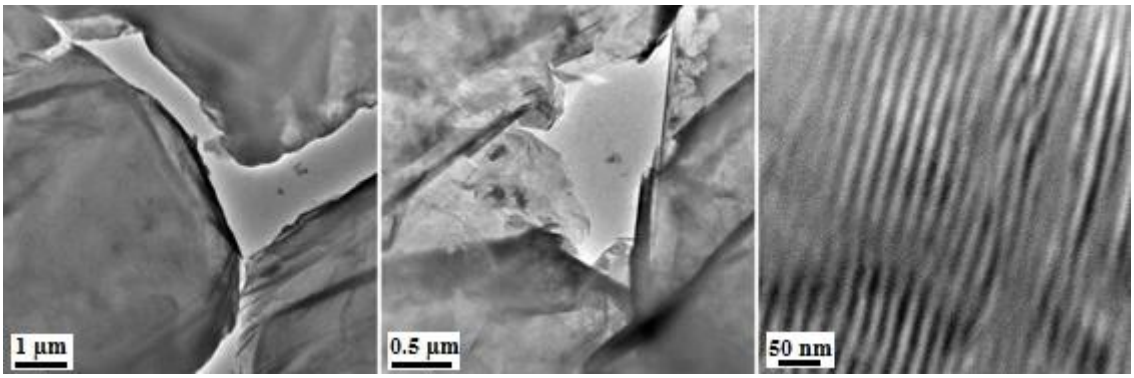

Fig. 4.5: TEM images of the biocomposites (1.5 wt % EG) at different magnifications.

4.4.4 Thermogravimetric analysis

The thermal stability is an important property of polymers that can limit their applications in uses. Thus, the thermal stability of the prepared samples was studied by TGA under nitrogen atmosphere and compared with the behavior of the pristine polymer.

Fig. 4.6 presents the TGA thermogram of the biocomposites and pristine polymer and Table 4.1 summarizes the results obtained. All the specimens showed thermal stability up to 205 °C. At this temperature less than 2 wt % loss observed which would be assigned to the evaporation of residual water.[26]

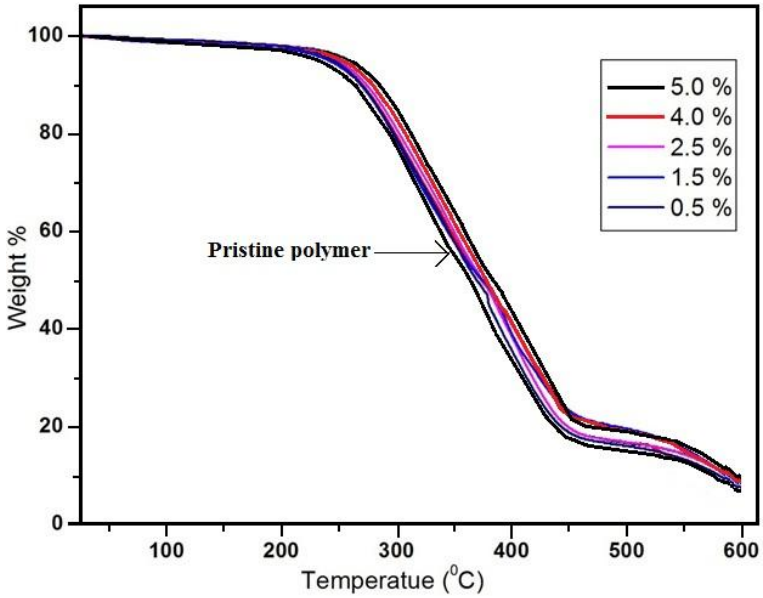

Fig. 4.6: TGA thermogram of the biocomposites with different wt % EG loading.

The thermal degradation of the biocomposites proceeds in two-stages. The first degradation occurs in the range of 205–243 °C and second in the range of 450–600 °C. The thermal stability of the biocomposites increases gradually with increasing concentration of EG. For instance, the initial degradation temperature for the neat polymer was observed at 205 °C and enhanced to 212 °C with 0.5 wt % EG loading and finally reached to 243 °C for the biocomposite with 5 wt % EG. The increase in thermo-stability of the biocomposites by the incorporation of EG can be explained by the reduced mobility of the polymer chains. As the degradation of polymers starts with the free radical formation at the weak bonds, followed by radical transfer to adjacent chains via inter

chain reactions, the strong interfacial adhesion of the polymer matrix and EG suppressed the chain transfer reaction and delayed the degradation process.[27] Higher the concentration of EG in the composites more pronounced is the effect. Moreover, the incorporation of EG into the polymer networks acts as a mass transport barrier to the volatile products generated during decomposition which may enhance the overall thermal stability of the biocomposites.[28] In addition, the polymers chains are intercalated between the layers and galleries of expanded graphite and contributes to the overall thermal stability of the biocomposites. The weight residue of the biocomposites at 600 °C is observed to be increased with EG content (Table 4.1), 6% for the neat polymer, whereas 13% for the biocomposite with 5 wt % EG loading. It is probably due to the formation of carbon net structure (graphene and/or expanded graphite) in the composites.[29]

Table 4.1: Thermal degradation data for the alkyd/epoxy/EG biocomposites.

EG wt %	details of the decomposition temperature (°C)				residual
	T_i	T_m	$T_d^{10\%}$	$T_d^{50\%}$	wt (%)
0	~ 205	~ 427	275	370	6
0.5	~ 212	~ 440	280	376	8
1.5	~ 215	~ 447	284	380	9
2.5	~ 225	~ 455	287	385	10
4.0	~ 236	~ 473	292	389	11
5.0	~ 243	~ 478	297	396	13

T_i = initial degradation temperature. T_m = maximum pyrolysis temperature. $T_d^{X\%}$ = X% weight loss temperature.

4.4.5 Mechanical properties

The mechanical properties of pristine polymer and its composites reinforced with different weight percentage of unexpanded graphite (UG) and EG platelet concentrations are summarized in Table 4.2. From the table, it can be seen that both the biocomposites show higher tensile strength than the pristine polymer with decreased elongation at break (%).

Table 4.2: Mechanical properties of the biocomposite films.

filler loading	tensile strength (MPa)		elongation at break (%)	
(wt %)	UG*	EG	UG	EG
0	17	17	62	62
0.5	19	22	58	56
1.5	22	26	47	42
2.5	25	30	41	35
4.0	29	35	34	24
5.0	36	43	25	20

*UG = unexpanded graphite.

The variation of elongation at break and tensile strength with different weight percentage of filler content is represented graphically in Fig. 4.7. It is observed that elongation at break of the biocomposites decreases gradually with increasing filler concentration. Compared to alkyd/epoxy blend, the biocomposite reinforced with 5 wt %

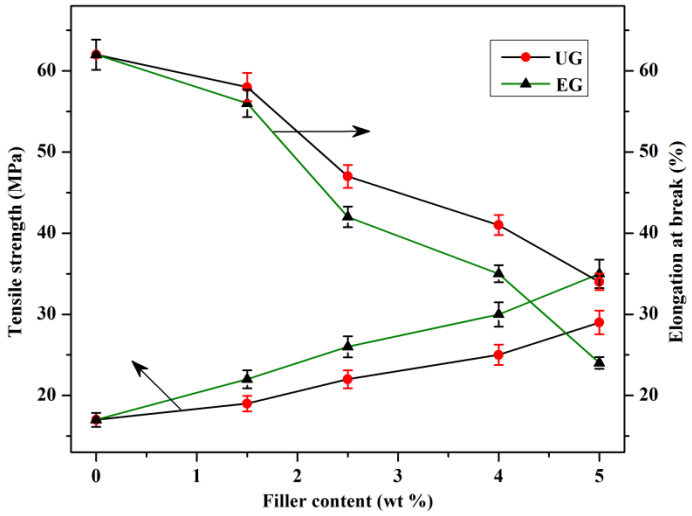

Fig. 4.7: Effects of UG and EG content on tensile strength and elongation at break (%) of the biocomposites.

UG platelets showed about 60% decrease in elongation at break, whereas it is decreased by 68% with same concentration of EG. It can be attributed to the strong interfacial interaction of the fillers and the polymer matrix, which restricts the mobility of polymer

chains.[27] The tensile strength of the biocomposites increases linearly with increasing filler concentration. For instance, the tensile strength of the alkyd/epoxy blend is 17 MPa, whereas the same increased by 5 MPa for the biocomposite with 0.5 wt % EG and finally reached to 43 MPa with 5 wt % EG loading. The improvement in tensile strength can be attributed to high strength and high aspect ratio of graphite platelets as well as to the homogeneous distribution and good interfacial adhesion between the platelets and the polymer matrix. All this characters provide efficient load transfer from the polymer matrix to the fillers and resulted in improved tensile properties of the biocomposites.[30] It is noticeable that compared to the pristine blend, the tensile strength for the biocomposite with 5 wt % EG increased by 153%, whereas it is increased by 112% with 5 wt % of UG. EG provide more surface area and functionalities like hydroxyl, carboxyl, aldehyde, ketone, ester, etc. which can better interact with the polar sites of the polymer matrix re and resulted in higher tensile strength than the unexpanded one.

4.4.6 *In vitro* degradation

In vitro degradation of the biocomposite was studied in phosphate buffer solution (PBS) by monitoring the weight loss during degradation. The degradation curves for the biocomposites with different wt % of EG are presented in Fig. 4.8. It was observed that

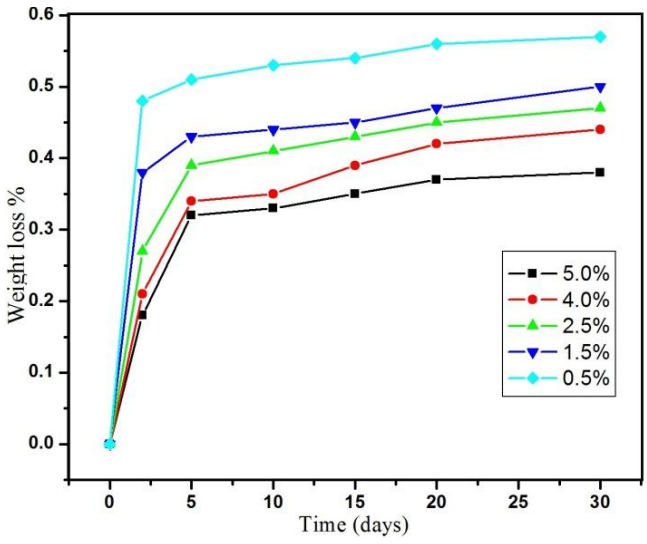

Fig. 4.8: Degradation curve of the biocomposites with different wt % of EG.

the weight loss of the biocomposite reaches a steady-state value in first five days. It may be due to some soluble substance present in the biocomposite. Afterward, due to the cross-linked polymer structure and overall hydrophobicity conferred by the long saturated hydrocarbon moieties in the biocomposite resist the degradation rate.[5] Moreover, incorporation of EG impart compactness and rigidity to the biocomposites and thereby resist the solvent penetration.

4.4.7 Water absorption

The water absorption behavior of the biocomposite was carried out to explore the potential applications of the biocomposite films. In general, water absorbance of a substance is affected by polarity and hydrophilicity of the functional groups present in the polymer. The biocomposite is hydrophobic because the fraction of amide groups is small and the hydroxyl groups are surrounded with aliphatic chains. In addition, −NH can form an intra-molecular hydrogen bond with a hydroxyl to decrease its hydrophilicity.[5] As a result of the high ester group content; it can also decrease the overall hydrophilicity in the biocomposite. At the same, expanded graphite present in the polymer matrix also enhancing the hydrophobicity. The hydrophobic nature of the biocomposite can be seen from Fig. 4.9. The water absorption decreases with increasing amount of EG content in

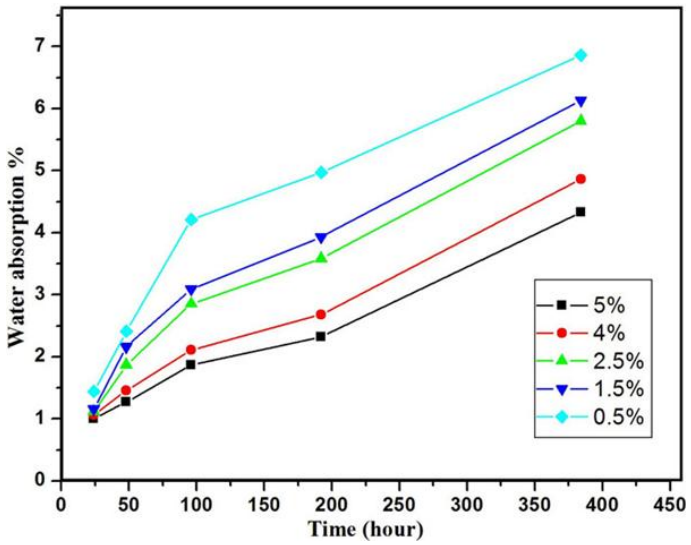

Fig. 4.9: Water absorption of the biocomposites with different wt % of EG.

the biocomposites. It can be attributed to the increased compactness and rigidity of the biocomposite structure with EG loading and thereby prevents the solvent penetration. It is observed that with the passes of time the water amount of water absorption slightly increases with decrease in the absorption rate.

4.4.8 Limiting oxygen index (LOI)

The LOI values obtained for the biocomposites with different weight percentage of EG and the pristine polymer are summarized in Table 4.3. The pristine blend, mainly composed of hydrocarbon chains, requires a very less amount of oxygen for the formation of flammable volatiles and propagation of flame and hence showed low flame retardancy (LOI value 18%). However, incorporation of only 0.5 wt % EG enhances the LOI value as 3% and increases gradually with increasing EG loading and finally it reaches the maximum (41%) when EG loading is 5 wt %. There is significant improvement of the flammability property. This can be attributed to the barrier property EG to heat and oxygen transport due to which ignition of the bio-composite delayed.[29]

Table 4.3: Limiting oxygen indices (LOI) and flaming characteristics of the composites.

EG wt %	LOI (%)	flame Description	smoke and fumes	char
0	18 (± 3.0)	candle like flame	small and dark	little
0.5	21 (± 2.0)	small and localized	small and dark	little
1.5	24 (± 2.0)	small and localized	small and dark	little
2.5	29 (± 1.0)	small and localized	small and dark	little
4.0	35(± 2.0)	small and localized	small and dark	little
5.0	41 (± 2.0)	small and localized	small and dark	higher

* Each value represents average three samples.

4.5 Conclusion

- EG is an effective filler to impart superior performance characteristics to the alkyd/epoxy resin matrix.
- The thermal stability of oil modified polymer matrix increased significantly (upto 38 °C) by the decoration of composite structure.
- Tensile strength of the alkyd/epoxy blend improved by more than 2.5 fold with 5 wt % EG loading.
- The homogeneous dispersion and strong interfacial adhesion of polymer matrix and EG platelets facilitates efficient load transfer from the polymer matrix to the fillers.
- The alkyd/epoxy/EG biocomposites also exhibited very low water absorption and PBS degradability.
- The flame retardant property of the polymer matrix improved significantly by the incorporation of EG.
- The prepared biocomposites has practical value and can find uses in surface coatings.

References

1. Li, F., & Larock, R.C. *J. Appl. Polym. Sci.* **84** (8), 1533–1543, 2002.
2. Kundu, P.P., & Larock, R.C. *Biomacromolecules* **6** (2), 797–806, 2005.
3. Ashraf, S.M., et al. *J. Appl. Polym. Sci*. **100** (4), 3094–3100, 2006.
4. Eren, T., & Kusefoglu, S.H. *J. Appl. Polym. Sci.* **97** (6), 2264–2272, 2005.
5. Wang, Z., et al. *Macromolecules* **45** (22), 9010−9019, 2012.
6. Diakoumakos, C.D., & Jones, F.N. *Surf. Coat. Technol.* **150** (1), 37–49, 2002.
7. Athawale, V.D., & Chamankar, A.V. *Pigm. Resin Technol.* **29** (6), 344-349, 2000.
8. Dutta, N., et al. *Prog. Org. Coat.* **49** (2), 146-152, 2004.
9. Yu, L., et al *Macromol. Symp.* **249** (1), 535-542, 2007.
10. Petersen, K., et al. *Starch* **53** (8), 356-361, 2001.

11. Bastoili, C. *Starch* **53** (8), 351-355, 2001.
12. Williams, G.I., & Wool, R.P. *Appl. Comp. Mat.* **7** (5-6), 421-432, 2000.
13. Kalaitzidou, K., et al. *Compos. Sci. Technol.* **67** (10), 2045-2051, 2007.
14. Zhao, Y.F., et al. *Compos. Sci. Technol.* **67** (11-12), 2528-2534, 2007.
15. Zheng, W., et al. *Polymer* **43** (25), 6767-6773, 2002.
16. Song, L.N., et al. *Compos. Sci. Technol*. **66** (13), 2156-2162, 2006.
17. Jin, J., et al. *Compos. Sci. Technol.* **70** (10), 1544-1549, 2010.
18. Uhl, F.M., et al. *Polym. Degrad. Stab*. **84** (2), 215-226, 2004.
19. Yasmin, A., et al. *Compos. Sci. Technol.* **66** (9), 1182–1189, 2006.
20. Boruah, M., et al. *Prog. Org. Coat.* **74** (3), 596-602, 2012.
21. Chen, G., et al. *Carbon* **41** (3), 619-621, 2003.
22. Si, Y., & Samulski, E.T. *Nano Lett.* **8** (6), 1679-1682, 2008.
23. Wu, X., et al. *Mater. Sci.* **45** (2), 483-489, 2010.
24. Dhakate, S.R., et al. *Int. J. Hydrogen Energy* **33** (23), 7146-7152, 2008.
25. Konwer, S., et al. *J. Mater. Sci.: Mater. Electron* **22** (8), 1154–1161, 2011.
26. Mincheva, R., et al. *Biomacromolecules* **14** (3), 890–899, 2013.
27. Mbhele, Z.H., et al. *Chem. Mater*. **15** (26), 5019-5024, 2003.
28. Gogoi, P., et al. *Prog. Org. Coat.* **84**, 128–135, 2015.
29. Konwer, S., et al *J. Electron Mater.* **40** (11), 2248-2255, 2011.
30. Yasmin, A., & Daniel, I.M. *Polymer* **45** (24), 8211–8219, 2004.
31. Iman, M., & Maji, T.K. *Carbohydr. Polym*. **89** (1), 290–297, 2012.